



Effect of expanded graphite particle size on the physical properties of compacted samples

S. Revo¹ · M. Melnichenko¹ · T. Avramenko¹ · K. Ivanenko¹ · P. Teselko¹

Received: 16 November 2018 / Accepted: 3 June 2019 / Published online: 8 June 2019
© King Abdulaziz City for Science and Technology 2019

Abstract

The compacted carbon samples were prepared with the help of the expanded graphite grinding. The different fractions were prepared using mechanical disintegration and separation of the powder. It was found that each fraction varies in its particles morphology which influences the powder internal elastic stresses, particles distribution, chaining and deposition in a cell. As a result, the anisotropy of electrical resistivity of the compacted expanded graphite reduces by the ~ 30%, when the dispersity of particles increases and their morphology tends to equiaxial. It was also shown that the expanded graphite with an average particle size of 120 μm has a high level of internal elastic stresses, an increased dislocation density and a significant lattice distortion. Therefore, the corresponding compacted samples have higher elastic characteristics and microhardness levels. The radial surface distribution of microhardness varies depending on the powder fraction in the compacted samples. It was found out that the values of microhardness are maximal in the central area of the samples. This may be caused by different densities of the compacted samples and different levels of the powder internal stresses.

Keywords Expanded graphite · Resistivity · Microstresses · Microhardness

Introduction

Transition from macro- to nano-structures induces changes in materials properties. This increases the scientific interest in development and improvement of methods for obtaining and studying nanomaterials. Carbon atoms are unique in that they are able to form many different kinds of bonds between them. This allowed scientists to discover a number of allotropic modifications of carbon materials that are actively studied in the modern material science. At the same time, the expanded graphite (EG) is one of the promising representatives of carbon nanomaterials (Sementsov et al. 2016; Mehra et al. 2018). It retains a number of physico-chemical properties of graphite and exhibits a good ability to compaction due to the branched nanostructural morphology. That is why the EG is now the most common material for manufacturing die-formed seals for valve stems, and other stuffing box applications (Roe and Torrance 2008). It is used not only for production of high-performance sealants, friction

units, flame retardants, insulation materials, but it can be also viewed as a raw material for other nanoscale forms of carbon, a filler of nanocomposite materials, an adsorbent of organic compounds (Avramenko et al. 2016), an alternative precursor for supercapacitors (Revo et al. 2013; Rachiy et al. 2015), etc. (Luo et al. 2017; Dong et al. 2018).

While developing new materials based on the EG and improving their processing technologies to assess the technical condition of the parts and to develop measures for their better performance, it is important to control the physical and mechanical properties of the material surface. Standard mechanical tests (tension, compression, bending) do not always help fully characterize the mechanical properties of new materials due to the small size of the samples and their insufficient plasticity at room temperature. Different methods of indentation are widely used to determine the physical and mechanical properties of fragile and low plastic materials (Miyoshi 2002). The influence of the EG particles dispersity and morphology on the surface distribution of microhardness in the compacted samples was analyzed in this work with the help of the continuous nanoindentation method.

✉ S. Revo
s_revo@i.ua

¹ Taras Shevchenko National University of Kyiv, 64/13,
Volodymyrska Street, Kiev 01601, Ukraine

Experimental

The EG powder was obtained by a rapid heating of the oxidized graphite in a cyclone-type furnace (Sementsov et al. 2016). Its specific surface area was $\sim 50 \text{ m}^2/\text{g}$, its bulk weight $-0.015 \text{ g}/\text{cm}^3$. The EG powder was mechanically grinded in a special two-pinion vertical disintegrator with mill a rotation speed of $2 \times 10^4 \text{ min}^{-1}$. The grinding was carried out for 30 min, after that the EG was separated into fractions ($50 \dots 260 \mu\text{m}$) using an automatic separation machine, which separated about 200 g of powder within 5 min.

Each EG fraction was compacted in a cylindrical press-form under a pressure of 30 MPa. The diameter of samples was 20 mm, the thickness was 2 mm.

The EG structure was studied using a scanning electron microscopy. The X-ray diffraction data were obtained with the help of an automatic diffractometer DRON-4 (CuK α radiation). The deep structure parameters (such as an average size of the coherent scattering blocks, a dislocation density for each fraction, microstresses) were estimated with an approximation method. The estimation of the resistivity anisotropy was carried out using a four-point measurement cell.

The microhardness of materials was measured at room temperature by a microindentation procedure on Micron-Gamma device. The “Micron-Gamma” apparatus provides a measure of the micromechanical characteristics of materials with the help of a continuous indentation, an indenter scanning (sclerometry), a metallography and a topography (Zaporozhets et al. 1993). The way to determine a level of the elastic deformation in the contact area according to the indentation data was thoroughly described in Galanov et al. (1999), as well as the methodology of treatment and analyzing of micro-indentation data (Oliver and Pharr 1992, 2004). The method of automatic immersion of the indenter allows the hardness, the contact elastic modulus and the Young’s modulus of the material to be determined. The results of micro-indentation of the compacted EG samples under loading (from 20 to 100 g) according to a simple “loading–unloading” scheme were analyzed and summarized in this work. Each series of injections included 15 consecutive indenter immersions with a step of $50 \mu\text{m}$. The movement of the indenter was measured with an accuracy of 1 nm.

Results and discussion

Previous investigations (Dovbeshko et al. 2005a, b; Sementsov et al. 2016) showed that the vermicular particles of the initial EG powder consist of a set of graphite

plates, the thickness of which varies from a few unit to several hundreds of nanometers, and the distance between them—of $10 \text{ nm} \text{--} 10 \mu\text{m}$. After grinding, the EG morphology was changed. The frame of the worm-like particles was destroyed and their fragmentation on scales was carried out. The EG with a dispersity of $260 \mu\text{m}$ were separate elements of the initial particles or small plates with ragged edges. The shape of the particles with an average size of $\sim 50 \mu\text{m}$ was closer to the discoid (Fig. 1a, b). Due to the EG structural features, the tendency towards delamination and orientation of the particles perpendicular to the pressing direction was observed under compacting. The formation of the structural anisotropy took place (Fig. 1c, d).

The X-ray studies indicated that parameters of the EG powder fine structure were changed after its grinding (Revo et al. 2017). The values of microstresses (P_{II}) for different EG fractions are given in Table 1. The maximum microstress values were observed for the EG particles with an average size of $120 \mu\text{m}$. This is due to the defects increase that occurs during slipping and destroying of graphite planes. After reaching the critical value of microstresses, the local processes of particles destruction change and further grinding leads to a decrease in the residual internal stresses of the powder.

Under pressure, the powder compacting smoothly ended in particles delamination on flakes. Most of the flakes were set and oriented in planes perpendicular to the pressing direction. The different morphology of the dispersed EG particles affected the degree of structure anisotropy of the compacted samples. This was confirmed by the anisotropy of the electrical resistivity. Figure 2 demonstrates the correlation between the difference in electrical resistivity and the dispersity of the particles. The resistivity was measured in two mutually perpendicular directions in relation to the compression direction of the samples. The anisotropy of electrical resistivity was estimated as the difference $\Delta\rho = \rho_{||} - \rho_{\perp}$, where $\rho_{||}$ is the resistivity along the pressing direction, and ρ_{\perp} is the resistivity in perpendicular direction.

When the particles dispersity increases and their morphology tends to equiaxial, the anisotropy of electrical resistivity of the compacted EG reduces by the $\sim 30\%$. This indicates the more isotropic samples structure and the lower particle ability to delamination.

Microindentation experiments of the EG samples have shown, that with an increase in the applied load the hardness decreases. Figure 3 demonstrates the correlation between the relative reduction of microhardness and the load changing. At the initial stages of loading up to 40 g the microhardness changes more dynamically. The further loading results in microhardness value close to equilibrium.

The microhardness of the initial EG decreases on 0.004 GPa with a load increasing from 20 to 30 g. The further increasing of the indentation force has little effect on this

Fig. 1 SEM images of EG powder with average particles size of 260 μm (a) and 50 μm (b) and compacted EG (with average particles size of 50 μm) along (c) and perpendicular (d) to the pressing direction

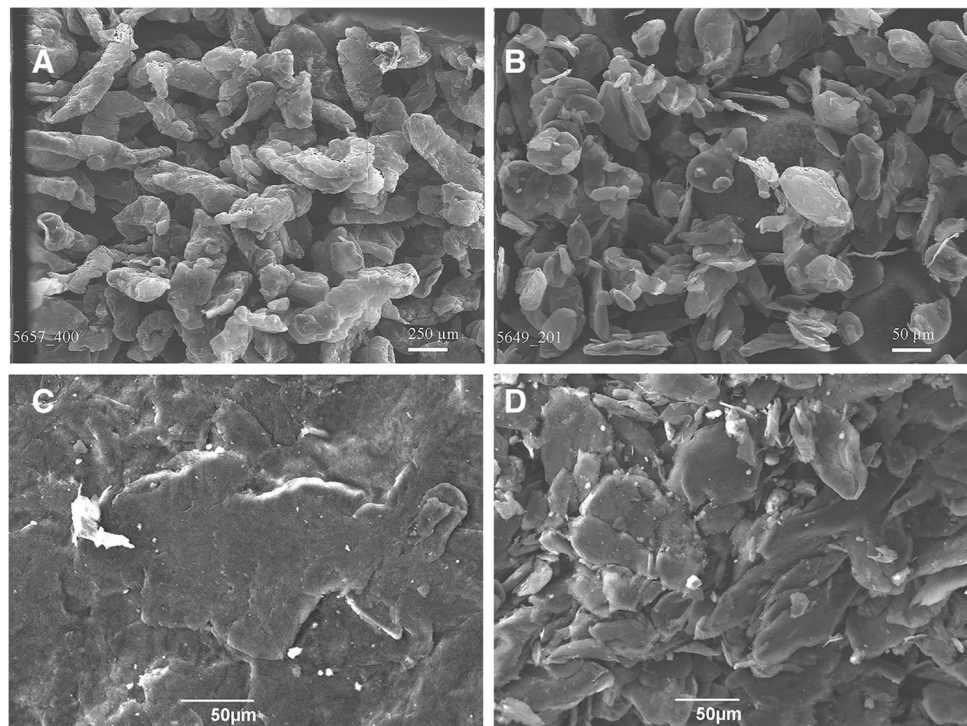


Table 1 Internal stresses of EG powder

Average particles size, μm	Microstresses, GPa
50	0.21
80	0.36
120	0.4
180	0.15
260	0.02
Initial EG	–

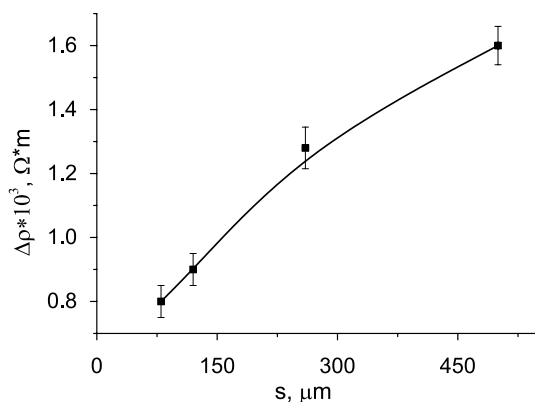


Fig. 2 The dependences of resistivity difference measured in two mutually perpendicular directions in relation to the pressing direction vs EG dispersity

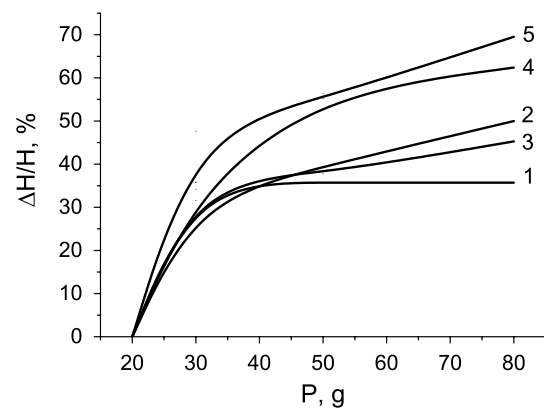


Fig. 3 The dependences of relative reduction of microhardness for compacted samples of initial EG (1) and average particle size s (μm)=50 (2), 80 (3), 120 (4), 180 (5) vs applied load

process. The microhardness of the EG particles with an average particles size of 180 μm decreases from 0.15 to 0.04 GPa.

At the same time, the value of microhardness increases with an increasing of a particle size up to $s = 120$ μm. However, for a larger particle size, it decreases. This is shown in Fig. 4: the microhardness of the EG samples with $s = 50$ μm is 0.019 GPa. For the EG with $s = 80$ and $s = 120$ μm, it equals 0.029 GPa and 0.044 GPa, respectively. The value of microhardness equals 0.035 and 0.009 GPa for particles dispersity of 180 μm and the initial EG.

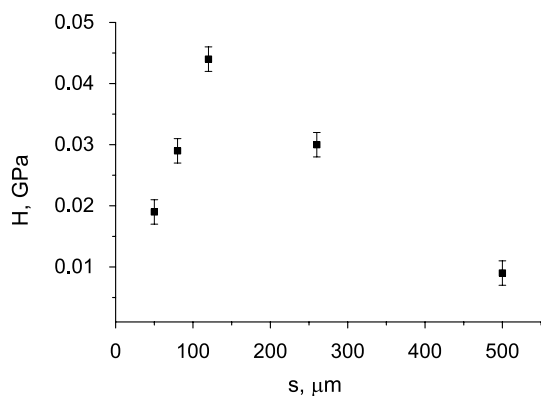


Fig. 4 Microhardness dependence vs powder dispersity for compacted EG samples under indentation load of 80 g

It was shown that the EG with an average particle size of 120 μm has a high level of internal elastic stresses, an increased dislocation density and a significant lattice distortion. Therefore, the corresponding compacted samples have increased elastic characteristics and a higher microhardness level.

An analysis of the microhardness distribution on the EG samples surface was also carried out. The surface of each

sample was divided into three equal parts and measurements were held along concentric circles having radii $1/4R$, $1/2R$ and $3/4R$, respectively. R is the radius of the sample. The change of the angular coordinate (azimuth) was observed during an indenter moving in a clockwise direction and the microhardness of the samples was measured. Figures 5, 6 and 7 demonstrate the microhardness indicatrix for the initial EG samples and those with an average particle size of $s = 180$ and $s = 50$ μm. The distribution of microhardness for the initial EG (Fig. 5) shows that the microhardness of the material decreases with the radial indenter displacement from the center of the sample. So, in the central part of the disk-shaped sample the values of microhardness are within the range from 0.04 to 0.025 GPa; whereas, in the next concentric area the microhardness is reduced by 30% and reaches the value of (0.028...0.014) GPa (line b in Fig. 5). Closer to the edges the sample is more fragile, thus, even an insignificant mechanical interaction between the indenter and the surface results in the delamination of its individual parts. This creates difficulties in determining the depth of immersion of the indenter and in measuring the microhardness of the material.

When the dispersity of the EG particles changes, the pattern of the microhardness distribution also varies. The

Fig. 5 The distribution of microhardness on the surface of the compacted sample with initial EG. The contour “a” a measurement in the center of the sample, “b” a measurement on the “middle line of the sample”

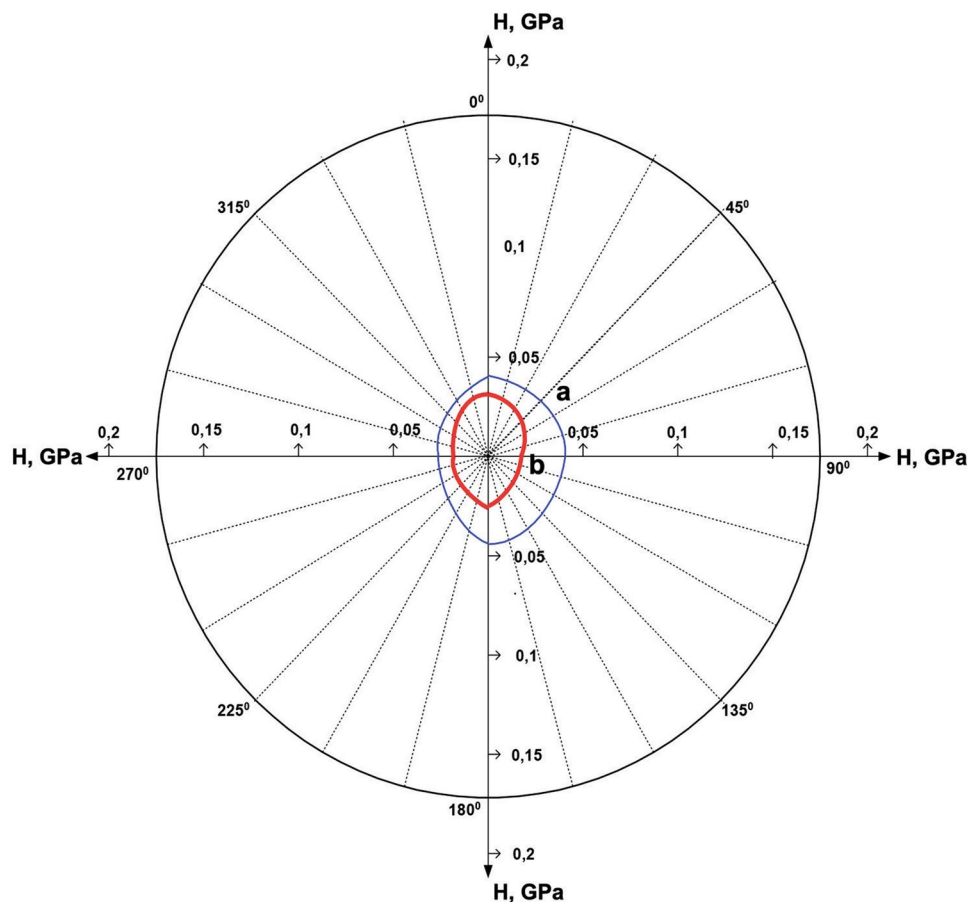
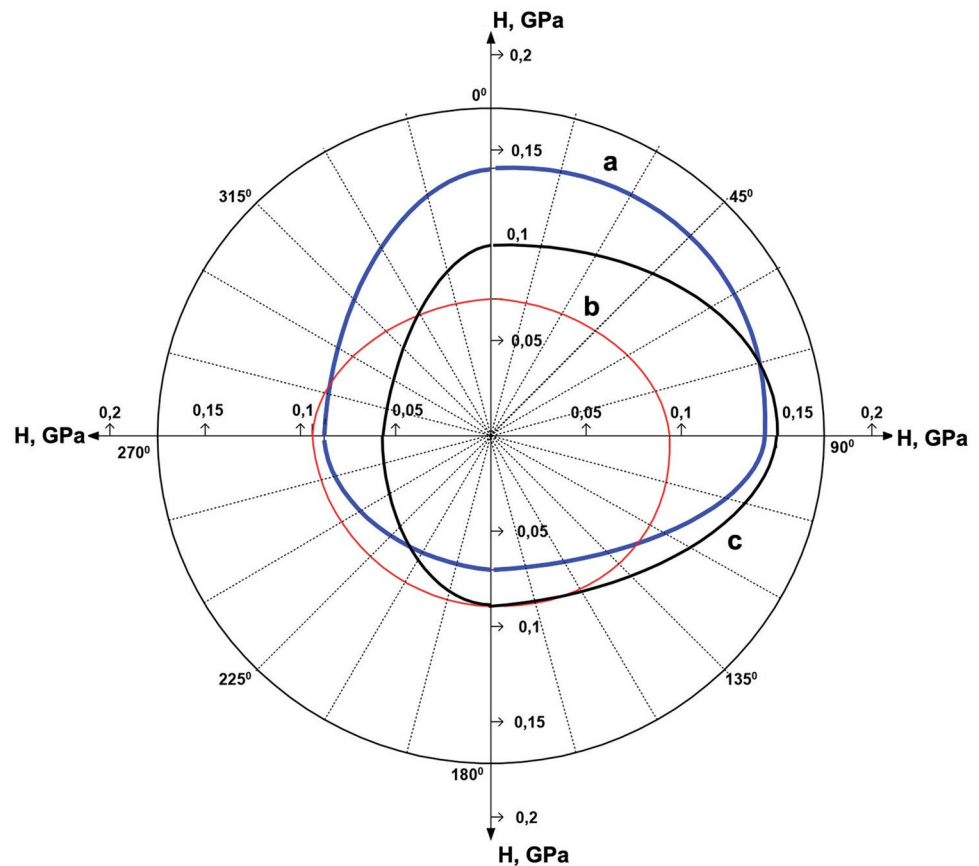


Fig. 6 The distribution of microhardness on the surface of the compacted sample with an average EG particles size of $180\ \mu\text{m}$. The contour “a” a measurement in the center of the sample, “b” a measurement on the “middle line of the sample”, “c” measurement at the edge of the sample



indicatrix of microhardness for the compacted EG sample with an average particle size of $180\ \mu\text{m}$ is shown in Fig. 6. In the center of the sample the value of microhardness (H) varies from 0.065 to 0.15 GPa. At the same time, in some sectors the value of H is almost 6 times higher than the corresponding values of microhardness obtained for the initial EG. Closer to the edge of the sample, the microhardness of the material decreases from 0.15 to 0.054 GPa.

The compacted EG sample with an average particle size of $50\ \mu\text{m}$ demonstrates an isotropic distribution of the microhardness values under the centered indentation and on the “middle line of the sample” (contour a and b Fig. 7). In this case, the values of H coincide for the central and medium concentric sample areas and equal ≈ 0.1 GPa. The absence of the contour “c” in Fig. 7 is caused by the difficulty of determining the microhardness of the sample closer to the edge due to the brittleness of the material.

The results of the microhardness surface distribution have shown that the values of microhardness are maximal in the central area of the samples. This may be caused by the different densities of compacted specimens and the level of the powder internal stresses. While manufacturing the samples the same technological conditions were kept. After filling the EG powder was evenly distributed in a cell space using a vibration method for a few seconds. However, the

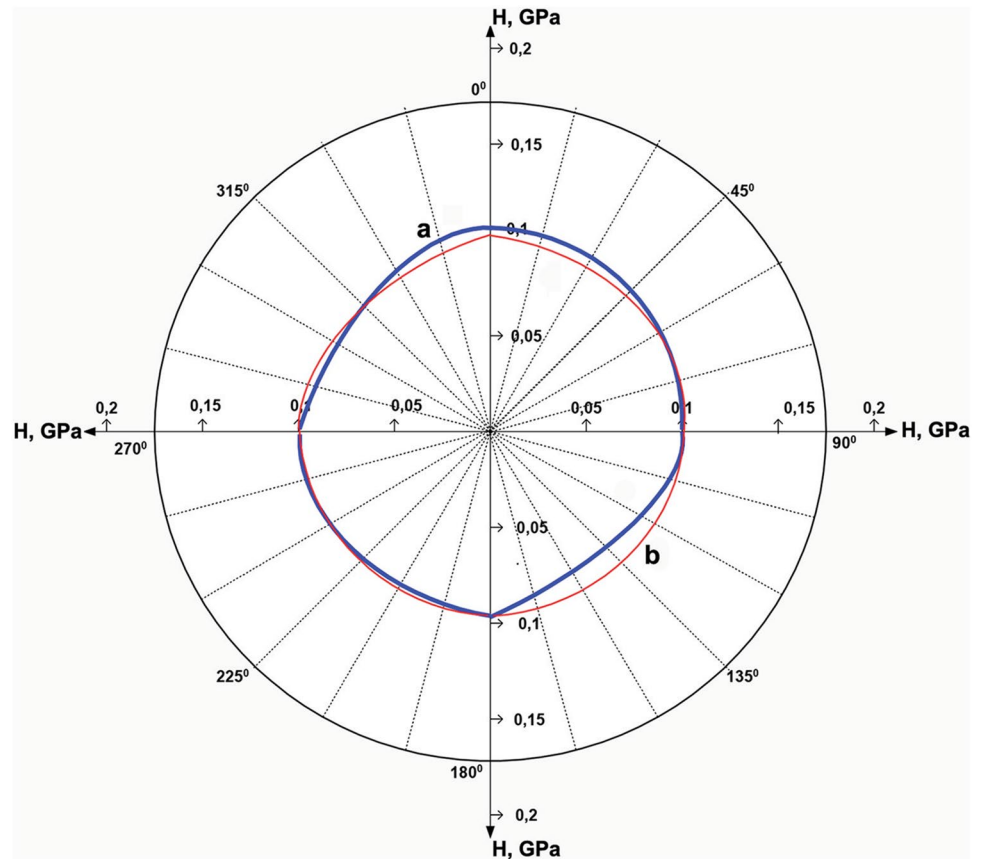
uneven distribution of the powder can be caused by the different morphology of its particles. The particles of the initial EG due to their vermicular and branched form can be well interconnected. Since there are no internal stresses in such powder, the increased value of microhardness in the central concentric area of the sample can be explained by the increased packaging density of the EG particles in this zone.

In the process of the EG grinding and reducing an average size of its particles up to $180\ \mu\text{m}$, internal stresses accumulate in the material. At the same time, with the change in the morphology of the particles, their aggregation capacity decreases, this affects the spatial distribution of the powder in the mold and the distribution packing density of the particle in the compacted sample.

The EG particles with a higher dispersity distribute more evenly in a cell space due to its morphological structure and more streamlined form. That is why there is an isotropic distribution of microhardness in such samples, the value of which depends on the level of the powder accumulated internal stresses.

Not only the change in an average particle size and its morphology, but also the change in internal residual stresses occurs during the EG grinding. This happens due to the kinetic processes taking place and the changing of the material defective structure during its grinding.

Fig. 7 The distribution of microhardness on the surface of the compacted sample with an average EG particles size of 50 μm . The contour “a” a measurement in the center of the sample, “b” a measurement on the “middle line of the sample”



Conclusion

In conclusion, the mechanical grinding of EG allows predictable changes in the morphology of the particles and optimizes the selection criteria of the grinded EG powder to improve the practically important characteristics of the EG-based nanocomposites. The proposed approach to the microhardness analysis gives an opportunity to characterize not only the micromechanical properties of the investigated material, but also to optimize the technological regimes for obtaining the samples. It should be noted that the higher values of hardness in the core of the compressed EG samples can provide a better structural strength of the construction components as a whole.

Compliance with ethical standards

Conflict of interest The authors declare that they have no competing interests.

References

- Avramenko TG, Khutoryanskaya NV, Mikhalyuk OV, Ivanenko EA, Revo SL (2016) Structure and sorption characteristics of nanoporous carbon materials. *J Surf Eng Appl Electrochem* 52:313–318. <https://doi.org/10.3103/S1068375516040037>
- Dong D, Jiang B, Li H, Du Y, Yang C (2018) Effect of graphite target power density on tribological properties of graphite-like carbon films. *J Appl Surf Sci* 439:900–909. <https://doi.org/10.1016/j.apsusc.2018.01.113>
- Dovbeshko GI, Gnatyuk OP, Nazarova AN, Sementsov YuI, Obraztsova ED (2005a) Vibrational spectra of carbonaceous materials: a SEIRA spectroscopy versus FTIR and raman. *Fuller Nanostruct Carbon Nanostruct* 13:393–400. <https://doi.org/10.1081/FST-200039387>
- Dovbeshko GI, Kopan' VS, Revo SL, Nishchenko MM, Prikhod'ko GP, Pyatkovs'ky ML, Sementsov YuI, Westermayer M (2005b) Nanostructure of exfoliated graphite. *J Metallofiz Noveishie Tekhnol* 27:1001–1010
- Galanov BA, Milman YuV, Chugunova SI, Goncharova IV (1999) Studies of mechanical properties of hard metals by indentation method. *J Superhard Mater* 3:25–38
- Luo Z, Huang Z, Xie N, Gao X, Xu T, Fang Y, Zhang Z (2017) Numerical and experimental study on temperature control of solar panels with form-stable paraffin/expanded graphite composite PCM. *J Energy Convers Manag* 149:416–423. <https://doi.org/10.1016/j.enconman.2017.07.046>
- Mehra NK, Jain AK, Nahar M (2018) Carbon nanomaterials in oncology: an expanding horizon. *J Drug Discov Today* 23:1016–1025. <https://doi.org/10.1016/j.drudis.2017.09.013>
- Miyoshi K (2002) Surface characterization techniques: an overview. Glenn Research, Center of NASA
- Oliver WC, Pharr GM (1992) An improved technique for determining hardness and elastic modulus using load and displacement

- sensing indentation measurements. *J Mater Res* 7:1564–1583. <https://doi.org/10.1557/jmr.1992.1564>
- Oliver WC, Pharr GM (2004) Measurement of hardness and elastic modulus by instrumented indentation: advances in understanding and refinements to methodology. *J Mater Res* 19:3–20. <https://doi.org/10.1557/jmr.2004.19.1.3>
- Rachiy BI, Budzulyak IM, Ivanenko EA, Revo SL (2015) A composite of nanoporous carbon and thermally exfoliated graphite as an effective electrode material for supercapacitors. *J Surf Eng Appl Electrochem* 51:501–508. <https://doi.org/10.3103/S1068375515050129>
- Revo SL, Budzulyak IM, Rachiy BI, Kuzishin MM (2013) Electrode material for supercapacitors based on nanostructured carbon. *J Surf Eng Appl Electrochem* 49:68. <https://doi.org/10.3103/S1068375513010122>
- Revo S, Avramenko T, Melnichenko M, Ivanenko K, Teselko P (2017) Morphological structure and microhardness of ground thermally expanded graphite. In: IEEE 7th international conference NAP. <https://doi.org/10.1109/NAP.2017.8190227>
- Roe M, Torrance A (2008) The surface failure and wear of graphite seals. *J Tribol Int* 41:1002–1008. <https://doi.org/10.1016/j.triboint.2008.03.006>
- Sementsov Yul, Revo SL, Ivanenko KO (2016) Thermally exfoliated graphite. Interservis, Kyiv
- Zaporozhets VV, Zakiev IM, Nikitin YuA (1993) Certificate of authorship USSR no 373581 (07 February, 1993)

Publisher's Note Springer Nature remains neutral with regard to jurisdictional claims in published maps and institutional affiliations.